

Simulated DW-MRI Brain Data Sets for Quantitative Evaluation of Estimated Fiber Orientations

Bryce Wilkins¹, Namgyun Lee^{1,2}, Meng Law^{1,3}, and Natasha Lepore^{1,4}

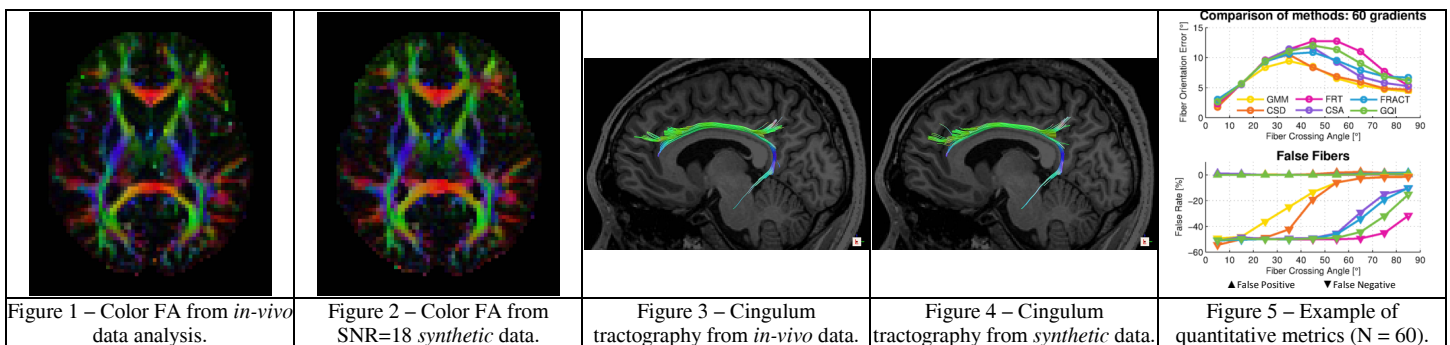
¹Biomedical Engineering, University of Southern California, Los Angeles, California, United States, ²Center of Magnetic Resonance Research, Korea Basic Science Institute, Ochang, Korea, ³Radiology, Keck School of Medicine of USC, Los Angeles, California, United States, ⁴Radiology, Children's Hospital of Los Angeles, California, United States

Target Audience: Researchers developing and/or evaluating DW-MRI fiber orientation estimation methods who need to quantitatively compare their results.

Purpose: As multi-fiber DW-MRI analysis is a relatively young field, much of the initial work has focused on development of new methods. Many approaches have been proposed with sometimes limited systematic comparison and, to our knowledge, no community-agreed-upon quantitative metrics. New methods are often introduced accompanied by simulation studies with comparison against a few alternatives, however differences in data synthesis, simulation parameters and/or evaluation metrics, usually prevents comparison to a broader range of similar work. Overall, it frequently remains unclear how new methods compare to existing approaches, and which method(s) yield the most accurate fiber estimations for a given data acquisition. These issues are increasingly important as studies involving brain networks and connectivity, which are frequently based on tractography derived from fiber estimation, become increasingly common. To address these concerns and encourage development of better methods, we created synthetic whole-brain DW-MRI data sets and quantitative tools for evaluating analyzed data. Analysis of a single-subject *in-vivo* data set provided a set of fiber orientations assumed as a ground-truth, which were subsequently used in a multi-tensor model for data synthesis. We generated synthetic DW data at SNRs of 9, 18 and 36, using sets of 20, 30, 40, 60, 90 and 120 gradient directions, and a diffusion-weighting of $b = 1000 \text{ s/mm}^2$ common to clinical acquisitions. The quantitative tools allow computation of estimated fiber orientation error, false-positive (spurious fiber) rates, and false-negative (missing fiber) rates. These data sets and quantitative tools are freely available on NITRC (www.nitrc.org) as the project "Simulated DW-MRI Brain Data Sets for Quantitative Evaluation of Estimated Fiber Orientations".

Methods: Development of ground-truth A DW data set was acquired by a twice-refocused pulsed-gradient spin-echo (PGSE) sequence with TE/TR = 83.4 ms/16100 ms, acquisition matrix = 128x128, ASSET acceleration factor of 2, voxel size = 2.4x2.4x2.4 mm, 60 contiguous slices, 150 diffusion gradient directions with diffusion-weighting $b = 1000 \text{ s/mm}^2$, and 10 non-diffusion weighted volumes. The data was processed by the probabilistic multi-fiber "ball and stick" method implemented as the program 'bedpostx' in the FMRIB Software Library (FSL)¹. Our synthetic DW data sets are derived from the fiber volume fractions (f_1, f_2, f_3) and orientations (v_1, v_2, v_3) estimated for each voxel by 'bedpostx'. Anatomical T1-weighted SPGR images (TE/TR = 2.856 ms/7 ms) were acquired with a voxel size of 1x1x1 mm. The anatomical volume was registered to the mean non-diffusion weighted volume and segmented into white-matter (WM), gray-matter (GM) and cerebrospinal fluid (CSF). The tissue classification map was used in assigning a tissue-specific diffusivity for the free-diffusion compartment in each voxel. Diffusion-weighted data synthesis Diffusion-weighted data were synthesized according to a multi-tensor model accommodating three crossing fibers per voxel in addition to a free-diffusion compartment. For any given voxel the signal model is: $S(b, g_j) = S_0[f_0 \exp(-bD_0) + (1 - f_0)\sum_k f_k \exp(-bg_j^T D_k g_j)]$ where S_0 simulates T2-weighting, f_0 and D_0 are the volume fraction and diffusivity, respectively, of the isotropic free-diffusion compartment, f_k and D_k are the volume fraction and diffusion tensor, respectively, of the k^{th} fiber in the voxel, b is the diffusion-weighting, and g_j is a unit vector representing the j^{th} gradient direction. Altogether the volume fractions satisfy $f_0 + (1 - f_0)\sum_k f_k = 1$. Each fiber's diffusion tensor, D_k , was computed by rotating a default single tensor, D_c . Complex Gaussian noise was added to the synthesized signal, S , to achieve a Rician distribution of noisy magnitude diffusion data. Quantitative metrics 1) Fiber orientation error is the angular separation between pairs of estimated and actual fiber orientations, and lies in the range 0–90°. 2) The number of incorrect fibers (either false-positives or false-negatives) was computed as the signed difference between the number of estimated and actual fibers (from the ground-truth) on a voxel-by-voxel basis. With this approach +1 indicates a single spurious fiber whereas -2 indicates two missing fibers.

Results: Approximately 250 voxels classified as WM and possessing FA values within [0.85, 0.95] in the *in-vivo* data were selected to determine the diffusivities $\{\lambda_1, \lambda_2, \lambda_3\} = \{1.70, 0.17, 0.17\} \times 0.001 \text{ mm}^2/\text{s}$ for the default single-fiber tensor D_c . The free diffusion parameter D_0 was computed for each tissue classification (WM, GM and CSF) separately by averaging diffusivities over similarly classified voxels, giving $\{D_0^{\text{WM}}, D_0^{\text{GM}}, D_0^{\text{CSF}}\} = \{0.68, 0.96, 2.25\} \times 0.001 \text{ mm}^2/\text{s}$. Diffusion-weighted data was generated according to the multi-tensor model using $N = 20, 30, 40, 60, 90$ and 120 gradient directions obtained from Camino². As an indication of the quality of the synthetic data, we illustrate the close correspondence of results obtained from *in-vivo* and synthetic data analysis. Figures 1 and 2 compare directional FA obtained by DTI analysis. Figures 3 and 4 illustrate tractography of the cingulum. Figure 5 shows quantitative results we obtained when comparing several well-known DW-MRI analysis methods (BSM⁴, CSD⁵, QBI⁶, FRAC⁷, CSA⁸, GQI⁹); the figure illustrates fiber orientation error and false fiber rates for voxels containing two fibers.



Discussion and Conclusion: Our synthetic data sets and quantitative metrics provide a means to systematically evaluate the performance of multi-fiber DW-MRI analysis methods in terms of metrics particularly relevant to tractography applications, including brain network and connectivity studies. We have illustrated the close correspondence between *in-vivo* and synthetic data analysis, which gives confidence in our simulation framework. The quantitative results provide an example of how the fiber estimation ability of several existing techniques can be compared, allowing selection of a best method for a given data acquisition. The data sets are provided at several SNR and gradient directions to allow the impact of each of these factors to be explored. The data and tools have been made publicly available on NITRC (www.nitrc.org), where we believe they can be utilized as a standardized test towards development of improved multi-fiber estimation methods, greater understanding of the relationship between existing methods, and ultimately have a positive impact on outcomes of diffusion data analysis.

References: 1. FSL: www.fmrib.ox.ac.uk/fsl 2. Camino: cmic.cs.ucl.ac.uk/camino 3. Behrens T, et al. Characterization and propagation of uncertainty in diffusion-weighted MR imaging. Magn. Reson. Med. 50 1077–1088 (2003) 4. Tournier J-D, et al. Robust determination of the fibre orientation distribution in diffusion MRI: non-negativity constrained super-resolved spherical deconvolution. NeuroImage 35 1459–1472 (2007) 5. Descoteaux M, et al. Regularized, fast, and robust analytical q-ball imaging. Magn. Reson. Med. 58 497–510 (2007) 6. Haldar J and Leahy R. Linear transforms for Fourier data on the sphere: Application to high angular resolution diffusion MRI of the brain. NeuroImage 71 233–247 (2013) 7. Aganj I, et al. Reconstruction of the orientation distribution function in single- and multiple-shell q-ball imaging within constant solid angle. Magn. Reson. Med. 64, 554–566 (2010) 8. Yeh F, et al. Generalized q-sampling imaging. IEEE Trans. Med. Imag. 29 1626–1635 (2010)